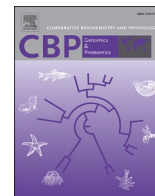




Contents lists available at ScienceDirect

Comparative Biochemistry and Physiology - Part D: Genomics and Proteomics

journal homepage: www.elsevier.com/locate/cbpd

Chromosome-level genome assembly of the European flat oyster (*Ostrea edulis*) provides insights into its evolution and adaptation

Xinchun Li^{a,1}, Yitian Bai^{a,1}, Zhen Dong^a, Chengxun Xu^a, Shikai Liu^a, Hong Yu^a,
Lingfeng Kong^a, Qi Li^{a,b,*}

^a Key Laboratory of Mariculture, Ministry of Education, Ocean University of China, Qingdao 266003, China

^b Laboratory for Marine Fisheries Science and Food Production Processes, Qingdao National Laboratory for Marine Science and Technology, Qingdao 266237, China

ARTICLE INFO

Edited by Chris Martyniuk

Keywords:

Ostrea edulis

Genome

Evolution

Transposable elements

Hox genes

ABSTRACT

The European flat oyster (*Ostrea edulis*) is an endangered and economically important marine bivalve species that plays a critical role in the coastal ecosystem. Here, we report a high-quality chromosome-level genome assembly of *O. edulis*, generated using PacBio HiFi-CCS long reads and annotated with Nanopore full-length transcriptome. The *O. edulis* genome covers 946.06 Mb (scaffold N50 94.82 Mb) containing 34,495 protein-coding genes and a high proportion of repeat sequences (58.49 %). The reconstructed demographic histories show that *O. edulis* population might be shaped by breeding habit (embryo brooding) and historical climatic change. Comparative genomic analysis indicates that transposable elements may drive lineage-specific evolution in oysters. Notably, the *O. edulis* genome has a *Hox* gene cluster rearrangement that has never been reported in bivalves, making this species valuable for evolutionary studies of molluscan diversification. Moreover, genome expansion of *O. edulis* is probably central to its adaptation to filter-feeding and sessile lifestyles, as well as embryo brooding and pathogen resistance, in coastal ecosystems. This chromosome-level genome assembly provides new insights into the genome feature of oysters, and presents an important resource for genetic research, evolutionary studies, and biological conservation of *O. edulis*.

1. Introduction

Oysters are filter-feeding and reef-engineer bivalve molluscs that are important to ecological system, fisheries and aquaculture (Bayne, 2017). With the rapid development of DNA sequencing technology in recent years, the genome sequences have been determined in several oyster species including four *Crassostrea* species (*Crassostrea gigas*, *C. virginica*, *C. hongkongensis* and *C. ariakensis*) and *Saccostrea glomerata* (Powell et al., 2018; Qi et al., 2021; Li et al., 2021a; Zhang et al., 2022). These genome resources are valuable for applied and fundamental basic research in oysters (Houston et al., 2020; Yang et al., 2020). However, very little is known about the genetic basis and evolutionary history of oysters in the genus *Ostrea*.

The European flat oyster *Ostrea edulis* represents an important aquaculture species native to the Atlantic and Mediterranean coasts of Europe (Fariñas-Franco et al., 2018; Colsoul et al., 2021). Although oyster aquaculture showed a steady increase in recent decades, *O. edulis*

has suffered a dramatic decrease in wild populations and aquacultural production due to adverse effects of climate change, overfishing, pollutants and diseases (Colsoul et al., 2021; Gilson et al., 2021). Moreover, this decline also had a negative impact on oyster reef habitats and posed a great challenge to the marine ecosystems (Beck et al., 2011). New genomic tools for breeding programs and management provide new opportunities to improve natural resources of *O. edulis* (Vera et al., 2019; Colsoul et al., 2021). Despite the construction of EST and mapping of SNPs in *O. edulis* over the past years (Pardo et al., 2016; Gutierrez et al., 2017), the detailed genome assembly and annotation have yet to be completed that are critical for ecological and evolutionary research as well as genetic exploitation of this species.

In the present study, we report a high-quality chromosome-level genome assembly for an *O. edulis* individual from the Netherlands, utilizing the Pacific Bioscience (PacBio) single-molecule sequencing and high-throughput chromosome conformation capture (Hi-C) technologies. Furthermore, Nanopore transcriptome sequencing was used to

* Corresponding author at: Key Laboratory of Mariculture, Ministry of Education, Ocean University of China, Qingdao 266003, China.

E-mail address: qili66@ouc.edu.cn (Q. Li).

¹ These authors contributed equally to this work.

<https://doi.org/10.1016/j.cbpd.2022.101045>

Received 31 August 2022; Received in revised form 17 November 2022; Accepted 25 November 2022

Available online 29 November 2022

1744-117X/© 2022 Elsevier Inc. All rights reserved.

improve the completeness of the genome annotation. Overall, the genome information reported here, as well as two recently co-published *O. edulis* genomes from the UK and French populations (the OEROSLIN_1.1 assembly and the Oe-Roscoff_1 assembly) (Boutet et al., 2022; Gundappa et al., 2022), will not only provide a better understanding of the genomic feature and evolutionary history of *O. edulis*, but also present new opportunities for research of conservation biology and genetic exploitation of this species.

2. Materials and methods

2.1. Sampling and sequencing

Farmed adult *O. edulis* were collected from Grevelingen and Oosterschelde in Netherlands (Fig. S1). The samples were dissected, immediately frozen in liquid nitrogen, and stored at -80°C for library preparation and further analysis. All these individuals were verified as members of *O. edulis* using DNA fragments of cytochrome oxidase I (COI) (Danic-Tchaleu et al., 2011).

Genomic DNA (gDNA) of a female *O. edulis* individual was extracted from adductor muscle and mantle for whole genome sequencing, using the standard phenol-chloroform method. For genome survey, short paired-end DNA reads from a whole genome sequence (WGS) library with insert size of 350 bp were produced using the Illumina NovaSeq 6000 system. For long-read sequencing, a PacBio library (15–20 kb) was prepared using the SMRTbell Express Template Prep Kit 2.0 following the CCS HiFi library protocol (Pacific Biosciences, CA). Single Molecule Real Time (SMRT) sequencing was conducted on a PacBio Sequel II sequencing platform using the SMRT Cell (8 M) and Sequel II Sequencing Kit 2.0. The subreads were filtered by minimum length of 50 kb, and the HiFi reads were generated using ccs software (version 4.2.0) with the parameters of “min-passes = 3, min-rq = 0.99” (<https://github.com/PacificBiosciences/ccs>). The adductor muscle of another *O. edulis* individual was fixed with 1 % formaldehyde and used for Hi-C library construction by following a procedure described previously (Rao et al., 2014). *Mbo*I was used as the restriction enzyme. The library was also sequenced on an Illumina NovaSeq 6000 platform.

Total RNA was isolated from different tissues including adductor muscle, digestive gland, gill, gonad, heart, hemolymph, labial palp and mantle from another *O. edulis* individual, using TRIzol reagent according to the manufacturer's instructions. Full-length (FL) transcriptome sequencing was performed using pooled RNA samples (in equal amounts) from seven tissues (adductor muscle, digestive gland, gill, gonad, heart, labial palp and mantle). The FL complementary DNA (cDNA) library was constructed using cDNA-PCR Sequencing Kit (SQK-PCS109) protocol from Oxford Nanopore Technologies (ONT), and then sequenced on the ONT PromethION platform with FLOPRO002 R9.4.1 flow cell using MinKNOW software (version 22.08.9). In addition, six short cDNA libraries with insert sizes of ~ 350 bp were prepared using RNA samples from six tissues (adductor muscle, gill, gonad, hemolymph, labial palp and mantle), and sequenced on Illumina NovaSeq 6000 system.

2.2. Genome survey, assembly, and scaffolding

Genome size, heterozygosity and repeat content were estimated based on k-mer analysis. Briefly, the quality control of the Illumina short reads was performed using fastp (version 0.23.1) (Chen et al., 2018). Distribution of 19-mer frequency was obtained using clean reads by Jellyfish software (version 2.2.10) (Marçais and Kingsford, 2011). Finally, the genome size, rate of heterozygosity and abundance of repetitive elements were estimated using the GCE software (version 1.0.0) (Liu et al., 2013).

The initial genome was assembled with hifiasm (version 0.16.1-r375) (Cheng et al., 2021) using HiFi reads following parameter “–purge-cov 39”. The Hi-C DNA reads were mapped to the initial

genome by Burrows-Wheeler Aligner (BWA) (version 0.7.17-r1198-dirty) (Li and Durbin, 2009) with default parameters, and the Hi-C contact matrix was constructed by Juicer software (version 1.6) (Durand et al., 2016) with default parameters. Subsequently, the correction of initial assembly errors and contig scaffolding were performed using 3D de novo assembly (3D-DNA) pipeline (version 180419) (Dudchenko et al., 2017) following parameters “–build-gapped-map –editor-repeat-coverage 5 –editor-coarse-resolution 50000 –editor-coarse-region 250000”. Finally, several slight manual corrections of the connections were performed in the Juicebox Assembly Tools (version 1.11.08) (Dudchenko et al., 2018) to ensure the scaffolds within the same pseudo-chromosomal linkage groups met the Hi-C linkage characteristics.

2.3. Genome assessment

Benchmarking Universal Single-Copy Orthologs (BUSCO) (version 5.3.2) (Manni et al., 2021) analysis was used to evaluate the completeness of gene coverage by searching against the BUSCO databases (metazoa_odb10 and mollusca_odb10). QUILT (version 5.0.2) (Gurevich et al., 2013) was used to check genome assembly quality with the raw PacBio HiFi reads. Moreover, the WGS short DNA reads of three *O. edulis* individuals from different sampling sites (Table S1) were mapped to the assembled genome by BWA (version 0.7.17-r1198-dirty) (Li and Durbin, 2009). The mapping rates were calculated based on the aligned file (.bam) using samtools software (version 1.15) (Li et al., 2009) to roughly assess the representative of our genome assembly. Additionally, to assess the accuracy of genome assembly, macrosynteny analysis was performed between our assembly and the other two *O. edulis* genome assemblies (the OEROSLIN_1.1 assembly and the Oe-Roscoff_1 assembly) (Boutet et al., 2022; Gundappa et al., 2022). Alignment plotting was conducted using D-GENIES software (version 1.3.0) (Cabannes and Klopp, 2018).

2.4. Genome annotation

The repetitive sequences in the *O. edulis* genome were annotated using both homology and de novo predictions. Briefly, RepeatModeler (version 2.0.1) (Flynn et al., 2020) was used to construct a de novo repeat library. Subsequently, the de novo library was combined with the data of molluscan repetitive sequences from Repbase library (version 20181026) (<https://www.girinst.org/repbase/>) and Dfam (version 3.3) (Wheeler et al., 2012). RepeatMasker (version 4.1.2-p1) (Tarailo-Graovac and Chen, 2009) was used to detect and classify repeat sequences in the genome with the combined library. The repeat landscape was generated using the accessory scripts calcDivergenceFromAlign.pl and createRepeatLandscape.pl available at the RepeatMasker package. Transposable element (TE) divergence analysis was made by using an R script modified from <https://github.com/ValentinaBoP/TransposableElements> with the detailed annotation table from the output of RepeatMasker.

Protein-coding gene prediction was performed by incorporating de novo prediction, homology-based, and transcriptome-assisted methods. For transcriptome-based prediction, short cDNA reads obtained from this study and downloaded from NCBI SRA database (SRA accession no. SRR16610371, SRR16610375) were first pre-processed by fastp (version 0.23.1) (Chen et al., 2018). Then, the clean reads were aligned to the *O. edulis* genome with HISAT2 (version 2.2.1) (Kim et al., 2015). Subsequently, the aligned file (.bam) was assembled by Trinity (version 2.14.0) (Grabherr et al., 2011) under a genome-guided mode. For de novo prediction, Augustus (version 3.4.0) (Stanke et al., 2008) was trained using Braker2 (version 2.1.5) (Brůna et al., 2021) with the soft-masked genome and transcriptome aligned file (.bam) of short cDNA reads. For homologous annotation, protein sequences of three well-annotated bivalves (*C. gigas*, *C. virginica* and *Mizuhopecten yessoensis*) were downloaded from the NCBI database. In addition, manually

annotated protein sequences (>50aa) of *Bivalvia* were downloaded from the Swiss-Prot database (Release 2022.1). A high confidence gene set was generated using Maker (version 3.01.03) (Cantarel et al., 2008) with the trained Augustus predictor, transcriptome assembly and protein sequences downloaded from NCBI and Swiss-Prot databases. To improve the gene structure annotation, we merged the gene set from Maker software (version 3.01.03) and gene models predicted with ONT FL transcriptome. Briefly, ONT cDNA reads were first filtered to remove the adapter sequences and low-quality raw reads (quality score less than 7), and then pre-processed by pypochopper (version 2.5.0) (<https://github.com/nanoporetech/pypochopper>) for the identification of FL reads, as well as trimming and orientation correction. Then, FL reads were mapped to genome using minimap2 (version 2.24-r1122) (Li, 2021). FL transcripts were assembled using StringTie2 (version 2.1.1) (Kovaka et al., 2019) in long read mode. Next, Transdecoder (version 5.5.0) (<https://github.com/TransDecoder/TransDecoder>) was used to identify candidate coding regions and predict gene models. Finally, gene models from Maker and ONT transcriptome-based prediction were combined using `agat_sp_merge_annotations.pl` script (<https://github.com/NBISweden/AGAT>).

Functional annotation of protein-coding genes was performed by homologous search against public databases. These include NCBI non-redundant protein (NR) (Release 2021_09_29) (Benson et al., 2000), Swiss-Prot (Bairoch and Apweiler, 2000), EggNOG (version 5.0) (Huerta-Cepas et al., 2019), Gene Ontology (GO) categories and Kyoto Encyclopedia of Genes and Genomes (KEGG) pathways (Kanehisa et al., 2017). In addition, gene motifs and domains were annotated using InterProScan (version 5.52-86.0) (Jones et al., 2014) against InterPro database (<https://www.ebi.ac.uk/interpro/>). The `pfam_scan.pl` script (<ftp://ftp.ebi.ac.uk/pub/databases/Pfam/Tools/PfamScan.tar.gz>) was used to align protein sequences against Pfam database (Pfam-A version 35.0) (Mistry et al., 2021).

Non-coding RNA (ncRNA) genes including transfer RNAs (tRNAs), microRNAs (miRNAs), ribosomal RNAs (rRNAs), and small nuclear RNAs (snRNAs) were annotated in the *O. edulis* genome. Briefly, tRNAs were predicted by tRNAscan-SE (version 2.0.7) (Chan et al., 2021) with parameters for eukaryotes. Screens for miRNAs, rRNAs and snRNAs were done using the Infernal (version 1.1.4) software (Nawrocki and Eddy, 2013) against the Rfam database (version 14.5) (Kalvari et al., 2018).

2.5. Effective population size estimation

The dynamics of effective population size (N_e) were estimated using the Pairwise Sequentially Markovian Coalescent (PSMC) (version 0.6.5-r67) software (Li and Durbin, 2011). The whole-genome sequencing data sets of a wild *O. edulis* from Bay of Morlaix in France and a wild Pacific oyster *C. gigas* from Dandong in China (Li et al., 2018) were downloaded from NCBI SRA database (SRA accession no. SRR17230313, SRR17226057, SRR6063159) (Table S1). Short DNA reads of *C. gigas* were mapped to the reference genome of Pacific oyster (Qi et al., 2021). The generation time (g) was assumed to be 1 year in both species, while mutation rates per nucleotide (μ) were set as $0.2e-8$ for both species (Li et al., 2021a).

2.6. Phylogenetic analysis, gene family expansion and contraction

The orthogroups (OGs) of 14 molluscan proteomes (Table S2) were identified using Orthofinder (version 2.5.2) (Emms and Kelly, 2019). OGs from selected molluscan taxa were used for subsequent phylogenetic analysis. The phylogenetic relationships between *O. edulis* and other species were inferred based on the 1043 shared single-copy orthologous genes. Sequence alignments were performed with MAFFT (version 7.475) (Katoh and Standley, 2013) under default parameters. Species tree was constructed using FastTree 2 (Price et al., 2010). Divergence time between species was estimated using MCMCTREE from

the PAML package (version 4.9j) (Yang, 2007). Eight reference-calibrated time points (Table S3) obtained from TimeTree database (<http://timetree.org/>) (Kumar et al., 2017) were used to constrain the nodes in the MCMC tree.

Gene family expansion and contraction were evaluated using CAFE (version 5) (Mendes et al., 2020) on the basis of the results from Orthofinder software (version 2.5.2) and species divergence time. A conditional P value was calculated for each gene family, and families with P value less than 0.05 were considered as having undergone significant expansion or contraction. GO enrichment and KEGG enrichment were performed for further functional analysis of expanded gene families, using the clusterProfiler R package (Yu et al., 2012).

2.7. Synteny analysis

The longest coding DNA sequences (CDS) for each gene, along with their coordinates, were prepared for five oyster species with chromosome-level assemblies (*O. edulis*, *O. denselamellosa*, *C. gigas*, *C. ariakensis*, and *C. virginica*). Next, pairwise comparisons were performed using MCScanX in the JCVI toolkit (version 1.1.12) (<https://github.com/tanghaibao/jcvi>) (Wang et al., 2012) to identify and visualize macrosynteny.

2.8. Homeobox gene analysis

The homeobox (*Hox*) genes were identified in both our *O. edulis* genome assembly and the OEROSLIN_1.1 assembly (Gundappa et al., 2022) by BLAST with an E -value threshold of $1e-10$ against *Hox* genes in *M. yessoensis* (Wang et al., 2017) and *Lottia gigantea* (Simakov et al., 2013) genomes, respectively. The data were further confirmed by comparing to the Conserved Domains Database (<http://www.ncbi.nlm.nih.gov/cdd>). Genes were classified based on BLAST results and molecular phylogeny. The same approach was also used to identify homeobox genes in other molluscan genomes (*Pomacea canaliculata*, *S. glomerata*, *O. denselamellosa*, *C. gigas*, *C. ariakensis* and *C. virginica*). Phylogenetic trees were constructed by IQ-TREE (version 2.1.4-beta) (Minh et al., 2020), based on sequence alignments by MAFFT (version 7.475) (Katoh and Standley, 2013).

3. Results and discussion

3.1. Genome assembly and annotation

Based on Illumina sequencing data (Table S4) and 19-mer analysis, the estimated genome size of *O. edulis* is around 913 Mb with high heterozygosity of 0.78 % and repeat content of 55.85 % (Table S5). Due to remarkable genetic heterozygosity or polymorphisms, genome sequencing and assembly were inherently challenge for molluscs (Sigwart et al., 2021). To obtain a high-quality genome, we sequenced 30.44 Gb ($\sim 33\times$) of PacBio HiFi long reads with an average length of 17.52 Kb (Table S4). These data were de novo assembled into 666 contigs with a N50 length of 3.23 Mb. With the aid of 132.06 Gb Hi-C data ($\sim 145\times$) (Table S4), the initial assembled contigs were anchored onto 10 chromosomes (Fig. S2), consistent with the haploid karyotype of *O. edulis* (Thiriot-Quievreux and Insua, 1992). Finally, a chromosome-level *O. edulis* genome assembly consisting of 618 scaffolds spanning 946.06 Mb is generated, with a scaffold N50 length of 94.82 Mb (Fig. 1A, Table 1, Table S5). The genome size of final assembly matched closely with our genome-size estimation by k-mer analysis and the OEROSLIN_1.1 assembly from the UK population (935.1 Mb) (Gundappa et al., 2022). The genome size of 946 Mb was slightly smaller than the 1.14 Gb genome size based on the flow cytometry results from the Spanish population (Rodríguez-Juiz et al., 1996) and the Oe-Roscoff_1 assembly (1.036 Gb) from the French population (Boutet et al., 2022). This discrepancy may be explained by population differences in genome size and high heterozygosity of *O. edulis*, which has been observed in

other bivalve genomes, including *C. gigas* (Peñaloza et al., 2021; Qi et al., 2021) and *Mytilus coruscus* (Yang et al., 2021; Sun et al., 2021).

Evaluation of the genome sequence completeness was performed based on BUSCO analysis (database: metazoa_odb10 and mollusca_odb10), and resulted in values of 95.1 % and 96.5 %, respectively (Table 1, Fig. S3). Moreover, the high mapping rate of short DNA reads of *O. edulis* individuals from different sampling sites demonstrates the high representative and accuracy of the genome assembly (Table S1). Furthermore, much of the genome comprises a high proportion of syntenic sequences compared with the OEROSLIN_1.1 assembly and the Oe-Roscoff_1 assembly (Boutet et al., 2022; Gundappa et al., 2022) (Fig. S4). Taken together, these data indicate a high-quality chromosome-scale genome assembly of *O. edulis* from this study, providing a robust framework for further exploration of oyster biology.

A total of 58.49 % bases were identified as repetitive sequences in the *O. edulis* genome (Table S6, Fig. S5), which is similar to the OEROSLIN_1.1 assembly (57.3 %) and the Oe-Roscoff_1 assembly (55.1 %) (Boutet et al., 2022; Gundappa et al., 2022). For gene annotation, we predicted 34,495 protein-coding genes with 131,967 isoforms in *O. edulis* (Table 1, Table S7). Approximately, 32,238 genes (93.46 %) were functionally annotated based on known proteins in public databases (Table S8). The gene set of *O. edulis* is larger than most oyster species sequenced to date (Li et al., 2021a; Peñaloza et al., 2021; Powell et al., 2018; Qi et al., 2021; Zhang et al., 2022), but similar to that of Eastern oyster *C. virginica*. Among three *O. edulis* genome annotations, the number of predicted gene models in our in-house annotation (Table S7) is slightly less than that of the other two in-house genome annotations of *O. edulis* (Boutet et al., 2022; Gundappa et al., 2022).

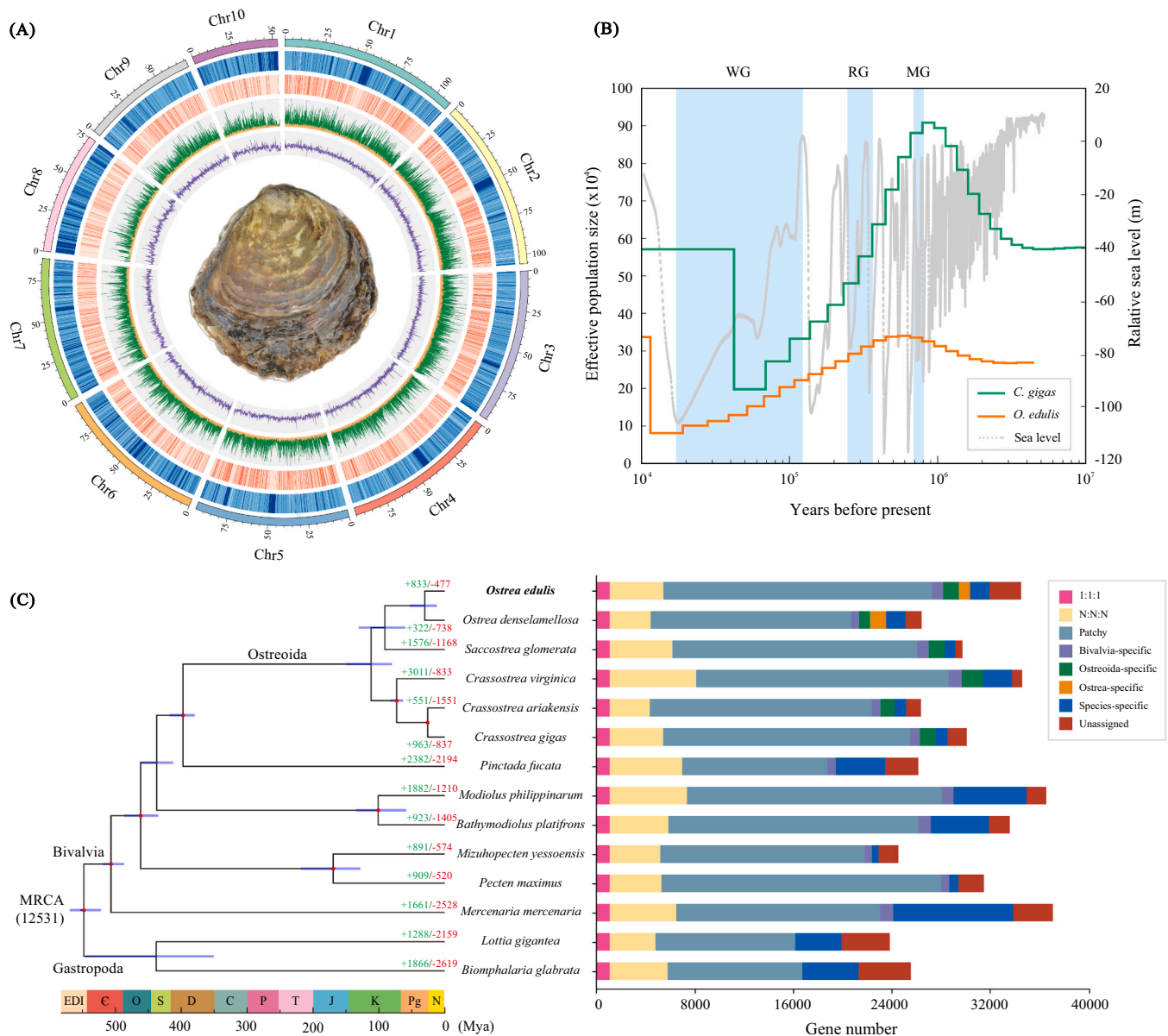


Fig. 1. The genome landscape and evolutionary history of *O. edulis*. (A) Circus plot of 10 chromosomes at 100-kb scale; with the European flat oyster at centre. From outer to inner ring are repeat coverage, the coverage of the longest CDS in each gene, the densities of isoforms (green) and genes (orange), and GC content. (B) Demographic histories of *O. edulis* and *C. gigas* inferred with the PSMC model. Estimates of the fluctuation of the global sea level relative to the present day were adopted from the literature (de Boer et al., 2014). (C) Phylogenetic tree and number of shared orthogroups among *O. edulis* and other molluscs. Reference-calibrated time points (Table S3) were indicated by red dots. The purple lines on the nodes indicate divergence time with a 95 % confidence interval. The numbers on each branch indicate gene family expansion (green) and contraction (red). C, Cambrian; C, Carboniferous; D, Devonian; EDI, Ediacaran; J, Jurassic; K, Cretaceous; Ma, million years ago; N, Neogene; O, Ordovician; P, Permian; Pg, Paleogene; S, Silurian; T, Triassic.

However, the average gene length of 16,913 bp and CDS length of 1406 bp in our annotation (Table S7) are longer than the average gene length (7411 bp) and CDS length (1224 bp) of the in-house annotation of the OEROSLIN_1.1 assembly (Gundappa et al., 2022). The average transcript length of our annotation (14,917 bp) (Table S7) is longer than that of the in-house annotation of the Oe-Roscoff_1 assembly (13,916 bp) (Boutet et al., 2022). Also, 95.1 % and 98.5 % of the complete BUSCOs (database: metazoa_odb10) could be covered by the gene set and isoform set, respectively (Table 1, Fig. S3). These results indicate a high completeness of the *O. edulis* genome annotation from this study. In addition, various ncRNA sequences were also identified and annotated in the genome, including 13,963 tRNAs, 86 miRNAs, 419 rRNAs and 335 snRNAs (Table S9). Recently, a NCBI RefSeq annotation of the OEROSLIN_1.1 assembly was completed and released (https://www.ncbi.nlm.nih.gov/genome/annotation_euk/Ostrea_edulis/100/). This new assembly predicted 38,526 gene models with the average gene length of 16,710 bp and average CDS length of 1866 bp. The NCBI RefSeq annotation of *O. edulis* is comprehensive including detailed annotation of pseudogenes and non-coding transcripts. Given that our transcriptome data were generated using the Nanopore Technology that give long sequence reads, our annotation could provide another valuable dataset to enhance the power and accuracy of genome based genetic and evolutionary studies in *O. edulis*.

3.2. Population history and phylogenetic analyses

Through reconstruction of the demographic history, we found that the *Ne* of *O. edulis* was estimated to be smaller than that of *C. gigas* throughout the Quaternary glaciations (2.58 Mya to present) (Fig. 1B). *O. edulis* exhibits brooding by fertilizing and incubating in the mantle cavity of females (Colsoul et al., 2021). The larvae of *O. edulis* have a relatively shorter planktonic dispersal stage compared with those of *C. gigas*, and tend to be more aggregated around the parent population (Guy et al., 2019). Therefore, it is possible that the reproductive strategy plays a potential role in limiting the rapid expansion of wild *O. edulis* population. In addition, both *O. edulis* and *C. gigas* were severely affected by glaciation events as their populations expanded in a stepwise manner before the Mindel glaciation (MG), and then experienced a rapid decline over the last two glacial periods, namely the Riss (RG, 0.24–0.37 Mya) and Würm (WG, 10–120 Kya) glaciation (Fig. 1B). Notably, the

Table 1
Summary statistics of assembly and annotation of *Ostrea edulis* genome.

| Feature | Statistics |
|---|------------------|
| Assembled genome size (Mb) | 946.06 |
| GC content (%) | 35.50 |
| Number of chromosomes | 10 |
| Number of scaffolds | 618 |
| Longest scaffold length (Mb) | 110.13 |
| N50 scaffold length (Mb); L50 scaffold count | 94.82; 5 |
| N50 contig length (Mb); L50 contig count | 3.23; 86 |
| Repeat content (%) | 58.49 |
| Gene number | 34,495 |
| Mean gene length (bp) | 16,913 |
| Number of single-exon genes | 3869 |
| Isoform number | 131,967 |
| Number of single-exon isoforms | 8138 |
| Genome complete BUSCOs/total BUSCOs ^a | 908/954 (95.1 %) |
| Genome other BUSCOs: S; D; F; M ^a | 898; 10; 6; 40 |
| Gene set complete BUSCOs/total BUSCOs ^{a,b} | 907/954 (95.1 %) |
| Gene set other BUSCOs: S; D; F; M ^{a,b} | 884; 23; 12; 35 |
| Isoform set complete BUSCOs/total BUSCOs ^a | 939/954 (98.5 %) |
| Isoform set other BUSCOs: S; D; F; M ^a | 119; 820; 10; 5 |

^a The lineage data set used for BUSCO assessment is metazoa_odb10 with 954 single-copy orthologues. S, Single-copy BUSCOs; D, Duplicated BUSCOs; F, Fragmented BUSCOs; M, Missing BUSCOs.

^b Gene set includes the annotated isoforms with the longest coding sequences and protein sequences.

population histories of the two oyster species show a remarkable correlation with the global sea-level fluctuation. For coastal marine species, sea-level drop caused by rapid cooling and glacier expansion have been viewed as a major cause of drastic decrease of available coastal habitat, resulting in genetic bottleneck, fragmented populations and population restructuring (Tsang et al., 2012; Ludt and Rocha, 2015; Li et al., 2021a). Hence, historical climatic change was potentially a main driver of demographic changes in oysters.

To infer the evolutionary history of *O. edulis*, a genome-wide phylogenetic tree was constructed based on 1043 single-copy genes from 14 molluscan genomes (Fig. 1C). The phylogenetic tree shows that *Ostrea* species and *S. glomerata* were inferred to diverge from the recent common ancestor around 91 Mya (60–130 Mya) (Fig. 1C), based on the secondary calibrations. During the Late Cretaceous period (66–100 Mya), oysters in both sides of the northern Atlantic Ocean became highly diversified, and a major burst of new genera occurred within a short period of time (Li et al., 2021b). Moreover, the divergence time of *O. edulis* from *O. denselamellosa* was dated to approximately 30 Mya (Fig. 1C), consistent with the diversity hotspot of oysters shifted from the Tethys to the Indian Ocean and East Asia from 66 to 23 Ma (Li et al., 2021b).

3.3. Genome structure characteristics

As observed in our genome assembly and the other two assemblies (Boutet et al., 2022; Gundappa et al., 2022), *O. edulis* has the larger haploid genome size than other previously sequenced oyster species (Table S10). High collinearity revealed by comparative genomic synteny among five oyster genomes (Fig. S6) suggests no whole genome duplication event in *O. edulis*. Comparing genome size with respect to the contents of transposons, CDS and Introns across six oyster species shows that TE content contributed to the majority of the differences across oysters (Pearson correlation $R^2 = 0.9071$, P -value = $3.34E-03$) (Figs. S7 and S8). Thus, the expansion of the genome size of *O. edulis* is mainly caused by proliferation of TEs.

TEs are considered as drivers of genetic innovation that have a considerable impact on the genome size and genome architecture (Feschotte and Pritham, 2007; Slotkin and Martienssen, 2007; Wang et al., 2021). The oyster genomes contain 41.06–57.27 % TEs (Table S11). Notably, a genomic feature of all oyster genomes is that TE landscape is dominated by DNA transposons (11.13–21.21 %) (Fig. 2A, Table S11). This is in agreement with previous reports of other molluscan genomes (Wang et al., 2017; Yan et al., 2019; Huang et al., 2022). In addition, *Helitrons* accounts for a substantial proportion of TEs in oyster genomes (Fig. 2A, Table S11). *Helitron* rolling-circle TEs are regarded as the remnants of past activity in the evolutionary history, and might shape the evolution of oyster genomes (Peñaloza et al., 2021). Kimura distance-based divergence analysis indicates that recent TE burst events generally contributed to highly dynamic repeat content of oyster genomes, and almost no recent *Helitron* expanded in the *O. denselamellosa* genome (Fig. S9). Interestingly, long interspersed nuclear element (LINE) and short interspersed nuclear element (SINE) are abundant in the genomes of *O. edulis* and *O. denselamellosa* (Fig. 2A, Table S11), and their bursts are found in both *Ostrea* species (Fig. S9). These results suggest the potential role of retrotransposons in driving *Ostrea* genome evolution. Moreover, a large proportion of the TEs in oyster genomes (5.69–18.10 %) are lineage-specific but unclassified (Fig. 2A, Table S11), which was also observed in the OEROSLIN_1.1 assembly (37.65 %) and the Oe-Roscoff_1 assembly (10.20 %) (Boutet et al., 2022; Gundappa et al., 2022). The unclassified lineage-specific TEs may be contributors towards the genome evolution of oysters. Collectively, these data indicate that oyster genomes have been strongly influenced by the activity of TEs, and consequently provide promising models for studying host-transposon interactions.

3.4. Hox cluster rearrangement

Hox genes are known for their critical roles in the early development of metazoans as they are involved in the patterning of the anterior-posterior body axis and segment identity (Ferrier and Holland, 2001; Holland, 2013; Gaunt, 2018). The genomic organization of Hox genes varies considerably across molluscs (Wanninger and Wollesen, 2019; Varney et al., 2021; Huang et al., 2022). Nevertheless, an intact cluster of 11 Hox genes was identified in *L. gigantea* (Simakov et al., 2013) and scallops (Li et al., 2017; Wang et al., 2017; Kenny et al., 2020), supporting an 11-gene Hox cluster in the molluscan ancestor. The ParaHox cluster, on the other hand, was considered to include 3 genes in another scaffold (Wang et al., 2017). In this study, we found that the *O. edulis* genome contains 10 Hox genes clustered in the same chromosome (Chr 4) and 3 ParaHox genes in another chromosome (Chr 2) (Fig. 2B, Fig. S10). *Antp* is missing from all six oyster genomes (Fig. 2B), which was considered as a potential driver of byssus formation (Zhang et al., 2022).

Strikingly, the anterior subcluster of *Hox1-Hox5* underwent a reverse transposition into *Hox5-Hox1*, located downstream of the original posterior subcluster *Lox5-Post1* in *O. edulis* (Fig. 2B). In addition, there is a large gap (8.3 Mb) between subclusters *Lox5-Post1* and *Hox5-Hox1*. Similar Hox cluster rearrangement was previously reported in the apple snail *P. canaliculata* (Sun et al., 2019). Since this is, to our knowledge, the first time that a bivalve's Hox gene cluster that differs from the pattern of molluscan ancestor, we performed the synteny analysis of genomic regions containing Hox genes (Fig. S11A-C) and confirmed the annotation of Hox gene cluster (Fig. S11D) in our assembly and the OEROSLIN_1.1 assembly (Gundappa et al., 2022). The transcription

directions of *Hox5* to *Hox1* genes also demonstrate the reverse transposition as well (Fig. 2B). With regards to the *ParaHox* gene cluster, *Gsx-Xlox* also has undergone a reverse transposition to become *Xlox-Gsx* in both *O. edulis* and *O. denselamellosa*, as indicated by the transcription directions (Fig. 2B). This result indicates that an inversion of *Gsx-Xlox* might exist in the common ancestor of *Ostrea* species. Large intra-chromosomal inversions among oyster genomes allow us to make inference that the reverse transposition of *ParaHox* and *Hox* genes is due to intra-chromosomal rearrangement (Fig. S6). This is in agreement with a previous report (Sun et al., 2019).

The clustered arrangement of Hox genes plays an important role in regulating gene expression (Wang et al., 2017; Gaunt, 2018). It has been suggested that subcluster temporal collinearity and dorsoventral decoupling of Hox gene expression could contribute to the evolution of molluscan novelties such as diverse body plans and shell formation (Wang et al., 2017; Huan et al., 2020; Zhang et al., 2021). Yet, it remains an open question as to whether variations in Hox expression are related to differences in genomic organization (Huan et al., 2020). Lineage-specific Hox cluster rearrangement was rarely found in bivalve genomes, and might be associated with potential evolutionary and biological innovations of *O. edulis*. Thus, the correlation between the genomic organization and expression of Hox genes in *O. edulis* can future studied to determine the regulatory mechanisms of molluscan Hox expression and the molecular basis underlying the diversification of molluscs.

3.5. Expanded and unique gene family analyses

Compared with other thirteen molluscan species, we identified 312

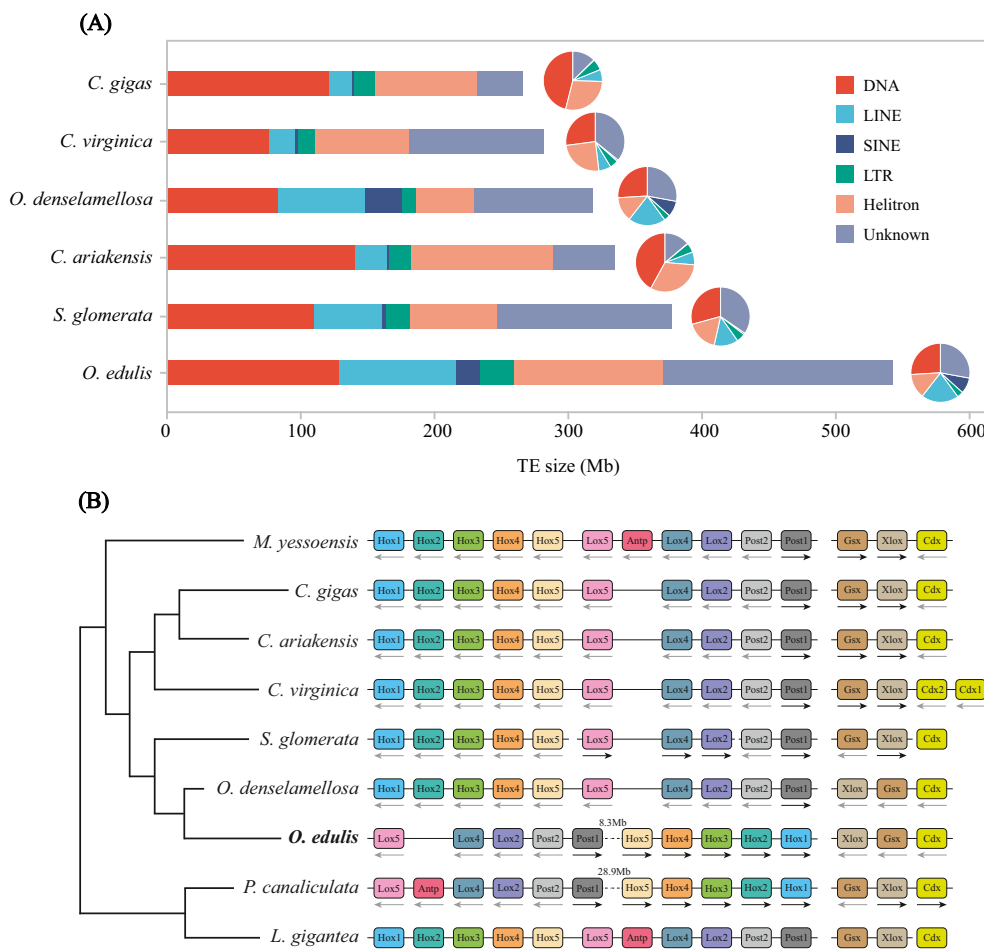


Fig. 2. Comparison of genome contents among oyster genomes. (A) Summary of TEs in six oyster genomes. Bar plots show the total TE size for each oyster genome partitioned according to the subfamily types. The pie charts indicate the proportions of DNA and Helitron transposons as well as LTR, LINE and SINE retrotransposons in each genome (the detail data is available in Table S11). (B) Hox and ParaHox gene clusters in *O. edulis* and eight other selected molluscs. Genes located on the same scaffold or chromosome are connected with a line but the line length has no proportion with their sequence length. Horizontal arrows denote transcription orientation.

expanded gene families, 78 contracted gene families and 430 species-specific gene families in *O. edulis*. Expanded genes were classified into 8 (KEGG BRITE) families associated with metabolism (cytochrome P450, lipid biosynthesis proteins, and glycosyltransferases), signaling and cellular processes (lectins, CD molecules, proteoglycans, glycosylphosphatidylinositol (GPI)-anchored proteins, and glycosaminoglycan binding proteins) (Fig. 3A, Table S12). KEGG pathway analysis indicates that genes involved in sensory system are expanded in the *O. edulis* genome (Fig. 3A). *O. edulis* keeps their offspring inside the female mantle cavity to protect them from external conditions, and tends to spend considerable energy during the brooding period (Mardones-Toledo et al., 2015). Furthermore, dead larvae may be detected by brooding oysters and ejected from the mantle cavity with pseudofeces (Chaparro et al., 2019; Gray et al., 2019). Genes related to lipid biosynthesis and sensory may be contributors towards metabolic regulation during brooding of embryos and enhancement of sensory capabilities in *O. edulis*. In addition, expanded and unique gene families are also enriched in KEGG pathways related to immune system, endocrine system, nervous system, xenobiotics biodegradation and metabolism, and signaling molecules (Fig. 3A, Fig. S12, Tables S13 and S14). GO enrichment analysis shows that expanded and unique gene families in *O. edulis* appear to be involved in immune responses such as xenobiotic metabolic process, and biosynthesis of antibacterial peptides (Figs. S13 and S14, Tables S15 and S16). Expansions of immune-related gene families has been previously described in two *O. edulis* genomes (Boutet et al., 2022; Gundappa et al., 2022) and other oysters (*C. gigas*, *C. virginica*, and *S. glomerata*) (Guo et al., 2015; Powell et al., 2018; Witkop et al., 2022), which plays an important role in adaptation to harsh environments. As a filter-feeder, *O. edulis* faces tremendous exposure to pathogenic microbes and rely solely on innate immunity for defense against pathogens. Therefore, expansion of immune-related

genes could contribute to the strong capability of *O. edulis* to thrive in microbe-rich environments.

Given the enrichment of immune-related genes in *O. edulis*, we further analyzed the expanded and unique gene families implicated in the immune defense of *O. edulis*, including cytochrome P450 (CYP450), lectins, complement C1q domain containing proteins (C1qDCs), fibrinogen-related proteins (FREPs), toll-like receptors (TLRs), multiple epidermal growth factor (MEGF) domain proteins, and protein groups associated with neuroendocrine immunomodulation (NEI) (Fig. 3B, Table S17). In mussels *Megaloniais nervosa* and *Dreissena polymorpha*, CYP450 gene families displayed a rapid expansion, which is considered as one of key drivers in adaptive evolution when facing multiple environmental challenges (Rogers et al., 2021; McCartney et al., 2022). Previous studies indicate that CYP450 protein homologs are linked to the biotransformation and detoxification of xenobiotics (Goldstone et al., 2006; Ertl et al., 2016). The expansion of CYP450 could result in a complex system for the generation and removal of ROS that is essential for immune and stress responses in oysters (Guo et al., 2015). It has been reported that in *C. virginica* and *Mercenaria mercenaria*, CYP450 are involved in response to parasite challenges (Tanguy et al., 2004; Perri-gault et al., 2009). Bonamiosis caused by the parasite *Bonamia ostreae*, which is an intracellular protozoan affecting *O. edulis* by infecting haemocytes, is currently the main focus for *O. edulis* production and a key factor driving its decline (Engelsma et al., 2014). Combined with previous studies (Morga et al., 2011; Pardo et al., 2016), CYP450 may participate in the defense of *B. ostreae*.

In bivalves, various pattern recognition receptors were combined to build immune recognition system (Wang et al., 2018a). Several expanded gene families associated with immune recognition have been identified in mussel and oyster genomes (Gerdol et al., 2011; Wang et al., 2018b; Gerdol et al., 2020). It is worth to note that the

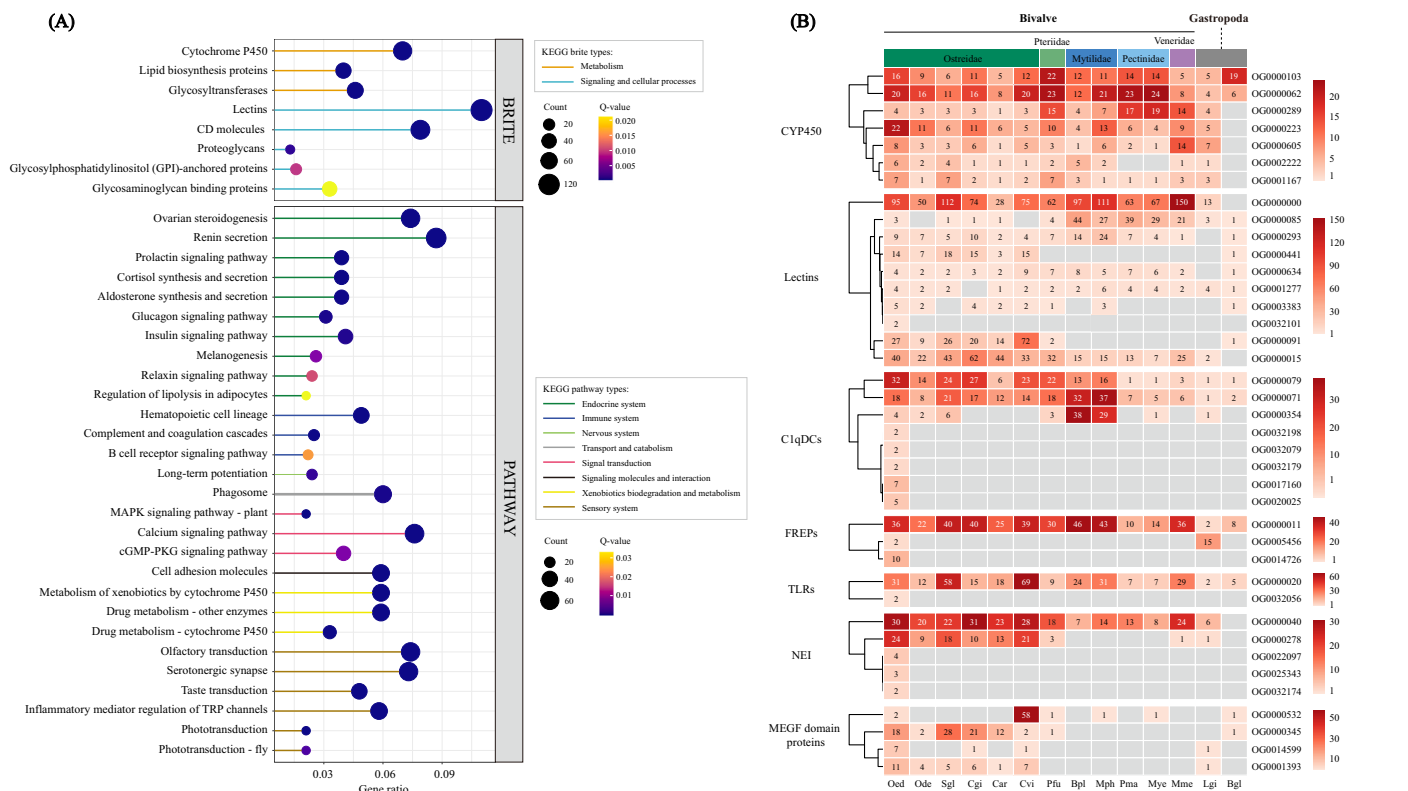


Fig. 3. Gene family expansions in key protein groups. (A) Enriched KEGG BRITE protein families and key pathways related to immune responses and embryo brooding derived from expanded gene families in *O. edulis* (the detail data is available in Table S12 and S13). (B) Immune-related expanded and unique orthologs in *O. edulis* (Oed) compared with thirteen molluscs, including *O. delamellosa* (Ode), *C. gigas* (Cgi), *C. ariakensis* (Car), *C. virginica* (Cvi), *S. glomerata* (Sgl), *P. fucata* (Pfu), *B. platifrons* (Bpl), *M. philippinarum* (Mph), *P. maximus* (Pma), *M. yessoensis* (Mye), *M. mercenaria* (Mme), *L. gigantea* (Lgi), and *B. glabrata* (Bgl) (the detail data is available in Table S17).

intraspecific genomic diversity of some pattern recognition receptors (C1qDCs, FREDs, and Ig domain-containing proteins) were among different populations revealed by the pan-genomic analysis of *M. galloprovincialis* (Gerdol et al., 2020). It is possible massive genetic variation associated to immune recognition may be linked to the evolutionary success in the environmental adaptation of marine invertebrates with high heterozygosity. Similar to our results (Fig. 3B), the expansions of gene families related to pathogen recognition (C-type lectins and C1qDCs) were also observed in another *O. edulis* genome assembly (Gundappa et al., 2022). *O. edulis* employs pattern recognition receptors, including lectins, TLRs and FREPs, as well as C1qDCs to detect pathogens and regulate innate immune responses during infection by *B. ostreae* (Pardo et al., 2016; Ronza et al., 2018; de la Ballina et al., 2021). Similarly, MEGF domain proteins are considered as pathogen recognition receptors and participate in immunological processes in *C. gigas* and *C. virginica* (Renault et al., 2011; Mcdowell et al., 2014; Chen et al., 2015). These expanded receptors in the canonical immune response pathways (Guo et al., 2015) and may enable *O. edulis* to develop a sophisticated innate immune system.

A previous report revealed a complete neuroendocrine-immune regulatory network in oysters, which could modulate immune response (Wang et al., 2018b). Recently, melanocyte-stimulating hormone (MSH) receptor was identified in *O. edulis* hyalinocytes, and might be able to mediate in bilateral information exchanges between the immune and neuroendocrine systems (de la Ballina et al., 2021). Therefore, expanded sets of neuronal acetylcholine receptor and MSH receptor (Fig. 3B, Table S17) could contribute to NEI regulatory network and play important roles in immune regulation in *O. edulis*. Taken together, these expanded and unique gene families related to innate immunity can provide important candidates for future investigations of disease resistance in *O. edulis*. Also, because of high heterozygosity rates in *O. edulis* genomes (Boutet et al., 2022; Gundappa et al., 2022), comparison of three genome assemblies from different populations will enrich our knowledge on the relationship of genetic variation and evolutionary adaptation of *O. edulis* in future.

4. Conclusions

Here, we present a chromosome-level genome assembly of *O. edulis* with high continuity (contig N50 length = 3.23 Mb, scaffold N50 length = 94.82 Mb), completeness (95.1 % complete metazoan BUSCOs) and accuracy. Demographic history and phylogenetic analyses reveal potential impacts of climate history and geological events on the evolution of *O. edulis*. Through comparative analysis of TE contents in oysters, we found that the large proportion of retrotransposons (LINE and SINE) likely contribute to *Ostrea*-specific evolution. Remarkably, like some gastropods but different from other bivalves examined, the *Hox* cluster is rearranged in *O. edulis*, with a reverse transposition of the ancestral anterior subcluster. Furthermore, key expansions of select gene families related to innate immunity may provide *O. edulis* with a genomic basis for strong innate immune system for disease resistance in *O. edulis*. This work advances our understanding of oyster evolution and provides valuable genomic resources for future basic research and biological conservation studies in this aquaculture and endangered species.

Supplementary data to this article can be found online at <https://doi.org/10.1016/j.cbd.2022.101045>.

Code availability

All codes and commands for the bioinformatics analyses carried out (using free softwares, as listed in the [Materials and methods section](#)) in the present study are contained in the supplementary file (Supplementary script).

Declaration of competing interest

The authors declare that they have no known competing financial interests or personal relationships that could have influenced the work reported in this paper.

Data availability

All raw genome and transcriptome sequencing data generated in this study have been deposited in NCBI under BioProject PRJNA846604. The whole-genome sequencing data were deposited with the SRA database under accession nos. SRR19578835-SRR19578837. The RNA-seq data have also been deposited with the SRA database under accession nos. SRR19578828-SRR19578834. The genome assembly and annotation data have been deposited in the CNGB Sequence Archive (CNSA) of the China National Gene Bank Database (<https://db.cngb.org/>) under accession no. CNP0003132 and Figshare database (doi:<https://doi.org/10.6084/m9.figshare.20013503>).

Acknowledgements

We acknowledge Laurel International Trade Co., Ltd. for their help in collecting the *O. edulis* samples from Netherlands. We thank Shaojun Du from the University of Maryland School of Medicine for assistance with grammatical editing in this manuscript. This work was supported by the grants from the China Agriculture Research System Project (CARS-49), and Earmarked Fund for Agriculture Seed Improvement Project of Shandong Province (2021LZGC027 and 2020LZGC016).

References

- Bairoch, A., Apweiler, R., 2000. The SWISS-PROT protein sequence database and its supplement TrEMBL in 2000. *Nucleic Acids Res.* 28 (1), 45–48. <https://doi.org/10.1093/nar/28.1.45>.
- Bayne, B.L., 2017. *Biology of Oysters*. Academic Press.
- Beck, M.W., Brumbaugh, R.D., Airolidi, L., Carranza, A., Coen, L.D., Crawford, C., Defeo, O., Edgar, G.J., Hancock, B., Kay, M.C., Lenihan, H.S., Luckenbach, M.W., Toropova, C.L., Zhang, G., Guo, X., 2011. Oyster reefs at risk and recommendations for conservation, restoration, and management. *Bioscience* 61 (2), 107–116. <https://doi.org/10.1525/bio.2011.61.2.5>.
- Benson, D.A., Karsch-Mizrachi, I., Lipman, D.J., Ostell, J., Rapp, B.A., Wheeler, D.L., 2000. GenBank. *Nucleic Acids Res.* 28 (1), 15–18. <https://doi.org/10.1093/nar/28.1.15>.
- Boutet, I., Alves Monteiro, H.J., Baudry, L., Takeuchi, T., Bonnard, E., Billoud, B., Farhat, S., Gonzales-Araya, R., Salaun, B., Andersen, A., Touleuc, J.-Y., Lallier, F., Flot, J.F., Guiguelmon, N., Guo, X., Allam, B., Pales-Espinoza, E., Hemmer-Hansen, J., Marbouty, M., Koszul, R., Tanguy, A., 2022. Chromosomal assembly of the flat oyster (*Ostrea edulis* L.) genome as a new genetic resource for aquaculture. *Evol. Appl.* <https://doi.org/10.1111/eva.13462>.
- Brüna, T., Hoff, K.J., Lomsadze, A., Stanke, M., Borodovsky, M., 2021. BRAKER2: automatic eukaryotic genome annotation with GeneMark-EP+ and AUGUSTUS supported by a protein database. *NAR Genom. Bioinform.* 3 (1) <https://doi.org/10.1093/nargab/lqaa108>.
- Cabanettes, F., Klopp, C., 2018. D-GENIES: dot plot large genomes in an interactive, efficient and simple way. *PeerJ* 6, e4958. <https://doi.org/10.7717/peerj.4958>.
- Cantarel, B.L., Korf, I., Robb, S.M.C., Parra, G., Ross, E., Moore, B., Holt, C., Alvarado, A. S., Yandell, M., 2008. MAKER: An easy-to-use annotation pipeline designed for emerging model organism genomes. *Genome Res.* 18 (1), 188–196. <https://doi.org/10.1101/gr.6743907>.
- Chan, P.P., Lin, B.Y., Mak, A.J., Lowe, T.M., 2021. tRNAscan-SE 2.0: improved detection and functional classification of transfer RNA genes. *Nucleic Acids Res.* 49 (16), 9077–9096. <https://doi.org/10.1093/nar/gkab688>.
- Chaparro, O.R., Mardones-Toledo, D.A., Gray, M.W., Cubillos, V.M., Navarro, J.M., Salas-Yanquin, L.P., 2019. Female-embryo relationships in *Ostrea chilensis*: brooding, embryo recognition, and larval hatching. *Mar. Biol.* 166 (1) <https://doi.org/10.1007/s00227-018-3457-1>.
- Chen, H., Wang, L., Zhou, Z., Hou, Z., Liu, Z., Wang, W., Gao, D., Gao, Q., Wang, M., Song, L., 2015. The comprehensive immunomodulation of NeurimmiRs in haemocytes of oyster *Crassostrea gigas* after acetylcholine and norepinephrine stimulation. *BMC Genomics* 16 (1). <https://doi.org/10.1186/s12864-015-2150-8>.
- Chen, S., Zhou, Y., Chen, Y., Gu, J., 2018. fastp: an ultra-fast all-in-one FASTQ preprocessor. *Bioinformatics* 34 (17), i884–i890. <https://doi.org/10.1093/bioinformatics/bty560>.
- Cheng, H., Concepcion, G.T., Feng, X., Zhang, H., Li, H., 2021. Haplotype-resolved de novo assembly using phased assembly graphs with hifiasm. *Nat. Methods* 18 (2), 170–175. <https://doi.org/10.1038/s41592-020-01056-5>.

- Colsoul, B., Boudry, P., Pérez Parallé, M.L., Bratoš Cetinić, A., Hugh Jones, T., Arzul, I., Mérout, N., Wegner, K.M., Peter, C., Merk, V., Pogoda, B., 2021. Sustainable large-scale production of European flat oyster (*Ostrea edulis*) seed for ecological restoration and aquaculture: a review. *Rev. Aquacult.* 13 (3), 1423–1468. <https://doi.org/10.1111/raq.12529>.
- Danic-Tchaleu, G., Heurtelbe, S., Morga, B., Lapegue, S., 2011. Complete mitochondrial DNA sequence of the European flat oyster *Ostrea edulis* confirms Ostreidae classification. *BMC Res Notes* 4, 400. <https://doi.org/10.1186/1756-0500-4-400>.
- de Boer, B., Lourens, L.J., van de Wal, R.S.W., 2014. Persistent 400,000-year variability of Antarctic ice volume and the carbon cycle is revealed throughout the Pliocene-Pleistocene. *Nat. Commun.* 5 (1) <https://doi.org/10.1038/ncomms3999>.
- de la Ballina, N.R., Villalba, A., Cao, A., 2021. Shotgun analysis to identify differences in protein expression between granulocytes and hyalinocytes of the European flat oyster *Ostrea edulis*. *Fish Shellfish Immunol.* 119, 678–691. <https://doi.org/10.1016/j.fsi.2021.10.045>.
- Dudchenko, O., Batra, S.S., Omer, A.D., Nyquist, S.K., Hoeger, M., Durand, N.C., Shamim, M.S., Machol, I., Lander, E.S., Aiden, A.P., Aiden, E.L., 2017. De novo assembly of the *Aedes aegypti* genome using Hi-C yields chromosome-length scaffolds. *Science* 356, 92–95. <https://doi.org/10.1126/science.aal3327>.
- Dudchenko, O., Shamim, M., Batra, S., Durand, N., Musial, N., Mostofa, R., Pham, M., Glenn St Hilaire, B., Yao, W., Stamenova, E., Hoeger, M., Nyquist, S., Korchina, V., Pletch, K., Flanagan, J., Tomaszewicz, A., McAloose, D., Estrada, C., Novak, B.J., Omer, A.D., Aiden, E., 2018. The Juicebox Assembly Tools module facilitates de novo assembly of mammalian genomes with chromosome-length scaffolds for under \$1000. *bioRxiv*. <https://doi.org/10.1101/254797>.
- Durand, N.C., Shamim, M.S., Machol, I., Rao, S.S.P., Huntley, M.H., Lander, E.S., Aiden, E.L., 2016. Juicer provides a one-click system for analyzing loop-resolution Hi-C experiments. *Cell Syst.* 3 (1), 95–98. <https://doi.org/10.1016/j.cels.2016.07.002>.
- Emms, D.M., Kelly, S., 2019. OrthoFinder: phylogenetic orthology inference for comparative genomics. *Genome Biol.* 20 (1) <https://doi.org/10.1186/s13059-019-1832-y>.
- Engelsma, M.Y., Culloty, S.C., Lynch, S.A., Arzul, I., Carnegie, R.B., 2014. Bonamia parasites: a rapidly changing perspective on a genus of important mollusc pathogens. *Dis. Aquat. Org.* 110 (1–2), 5–23. <https://doi.org/10.3354/dao02741>.
- Ertl, N.G., O'Connor, W.A., Brooks, P., Keats, M., Elizur, A., 2016. Combined exposure to pyrene and fluoranthene and their molecular effects on the Sydney rock oyster, *Saccostrea glomerata*. *Aquat. Toxicol.* 177, 136–145. <https://doi.org/10.1016/j.aquatox.2016.05.012>.
- Fariñas-Franco, J.M., Pearce, B., Mair, J.M., Harries, D.B., Macpherson, R.C., Porter, J.S., Reimer, P.J., Sanderson, W.G., 2018. Missing native oyster (*Ostrea edulis* L.) beds in a European Marine Protected Area: Should there be widespread restorative management? *Biol. Conserv.* 221, 293–311. <https://doi.org/10.1016/j.biocon.2018.03.010>.
- Ferrier, D.E.K., Holland, P.W.H., 2001. Ancient origin of the Hox gene cluster. *Nat. Rev. Genet.* 2 (1), 33–38. <https://doi.org/10.1038/35047605>.
- Feschotte, C., Pritham, E.J., 2007. DNA transposons and the evolution of eukaryotic genomes. *Annu. Rev. Genet.* 41, 331–368. <https://doi.org/10.1146/annurev.genet.40.110405.090448>.
- Flynn, J.M., Hubley, R., Goubert, C., Rosen, J., Clark, A.G., Feschotte, C., Smit, A.F., 2020. RepeatModeler2 for automated genomic discovery of transposable element families. *PNAS* 117 (17), 9451–9457. <https://doi.org/10.1073/pnas.1921046117>.
- Gaunt, S.J., 2018. Hox cluster genes and collinearities throughout the tree of animal life. *Int. J. Dev. Biol.* 62 (11–12), 673–683. <https://doi.org/10.1387/ijdb.180162sg>.
- Gerdol, M., Moreira, R., Cruz, F., Gómez-Garrido, J., Vlasova, A., Rosani, U., Venier, P., Naranjo-Ortiz, M.A., Murgarella, M., Greco, S., Balseiro, P., Corvelo, A., Frias, L., Gut, M., Gabaldón, T., Pallavicini, A., Canchaya, C., Novoa, B., Aliotti, T.S., Posada, D., Figueras, A., 2020. Massive gene presence-absence variation shapes an open pan-genome in the Mediterranean mussel. *Genome Biol.* 21 (1) <https://doi.org/10.1186/s13059-020-02180-3>.
- Gerdol, M., Manfrin, C., De Moro, G., Figueras, A., Novoa, B., Venier, P., Pallavicini, A., 2011. The Clq domain containing proteins of the Mediterranean mussel *Mytilus galloprovincialis*: A widespread and diverse family of immune-related molecules. *Dev. Comp. Immunol.* 35 (6), 635–643. <https://doi.org/10.1016/j.dci.2011.01.018>.
- Gilson, A.R., Coughlan, N.E., Dick, J.T.A., Kregting, L., 2021. Marine heat waves differentially affect functioning of native (*Ostrea edulis*) and invasive (*Crassostrea [Magallana] gigas*) oysters in tidal pools. *Mar. Environ. Res.* 172, 105497 <https://doi.org/10.1016/j.marenvres.2021.105497>.
- Goldstone, J.V., Hamdoun, A., Cole, B.J., Howard-Ashby, M., Nebert, D.W., Scally, M., Dean, M., Epel, D., Hahn, M.E., Stegeman, J.J., 2006. The chemical defensome: Environmental sensing and response genes in the Strongylocentrotus purpuratus genome. *Dev. Biol.* 300 (1), 366–384. <https://doi.org/10.1016/j.ydbio.2006.08.066>.
- Grabberr, M.G., Haas, B.J., Yassour, M., Levin, J.Z., Thompson, D.A., Amit, I., Adiconis, X., Fan, L., Raychowdhury, R., Zeng, Q., Chen, Z., Maudsli, E., Hacohen, N., Gnirke, A., Rhind, N., di Palma, F., Birren, B.W., Nusbaum, C., Lindblad-Toh, K., Friedman, N., Regev, A., 2011. Full-length transcriptome assembly from RNA-Seq data without a reference genome. *Nat. Biotechnol.* 29 (7), 644–652. <https://doi.org/10.1038/nbt.1883>.
- Gray, M.W., Chaparro, O., Huebert, K.B., O'Neill, S.P., Couture, T., Moreira, A., Brady, D. C., 2019. Life history traits conferring larval resistance against ocean acidification: the case of brooding oysters of the genus *Ostrea*. *J. Shellfish Res.* 38 (3), 751–761. <https://doi.org/10.2983/035.038.0326>.
- Gundappa, M.K., Peñaloza, C., Regan, T., Boutet, I., Tanguy, A., Houston, R.D., Bean, T. B., Macqueen, D.J., 2022. A chromosome level reference genome for European flat oyster (*Ostrea edulis* L.). *Evol. Appl.* <https://doi.org/10.1111/eva.13460>.
- Guo, X., He, Y., Zhang, L., Lelong, C., Jouaux, A., 2015. Immune and stress responses in oysters with insights on adaptation. *Fish Shellfish Immunol.* 46 (1), 107–119. <https://doi.org/10.1016/j.fsi.2015.05.018>.
- Gurevich, A., Saveliev, V., Vyahhi, N., Tesler, G., 2013. QUAST: quality assessment tool for genome assemblies. *Bioinformatics* 29 (8), 1072–1075. <https://doi.org/10.1093/bioinformatics/btt086>.
- Gutierrez, A.P., Turner, F., Gharbi, K., Talbot, R., Lowe, N.R., Peñaloza, C., McCullough, M., Prodöhl, P.A., Bean, T.P., Houston, R.D., 2017. Development of a medium density combined-species SNP array for Pacific and European oysters (*Crassostrea gigas* and *Ostrea edulis*). *G3 (Bethesda, Md.)* 7 (7), 2209–2218. <https://doi.org/10.1534/g3.117.041780>.
- Guy, C., Smyth, D., Roberts, D., 2019. The importance of population density and inter-individual distance in conserving the European oyster *Ostrea edulis*. *J. Mar. Biol. Assoc. U. K.* 99 (3), 587–593. <https://doi.org/10.1017/S0025315418000395>.
- Holland, P.W.H., 2013. Evolution of homeobox genes. *Wires Dev Biol.* 2 (1), 31–45. <https://doi.org/10.1002/wdev.78>.
- Houston, R.D., Bean, T.P., Macqueen, D.J., Gundappa, M.K., Jin, Y.H., Jenkins, T.L., Selly, S.L.C., Martin, S.A.M., Stevens, J.R., Santos, E.M., Davie, A., Robledo, D., 2020. Harnessing genomics to fast-track genetic improvement in aquaculture. *Nat. Rev. Genet.* 21 (7), 389–409. <https://doi.org/10.1038/s41576-020-0227-y>.
- Huan, P., Wang, Q., Tan, S., Liu, B., 2020. Dorsorostral decoupling of Hox gene expression underpins the diversification of molluscs. *PNAS* 117 (1), 503–512. <https://doi.org/10.1073/pnas.1907328117>.
- Huang, Z., Huang, W., Liu, X., Han, Z., Liu, G., Boamah, G.A., Wang, Y., Yu, F., Gan, Y., Xiao, Q., Luo, X., Chen, N., Liu, M., You, W., Ke, C., 2022. Genomic insights into the adaptation and evolution of the nautilus, an ancient but evolving “living fossil”. *Mol. Ecol. Resour.* 22 (1), 15–27. <https://doi.org/10.1111/1755-0998.13439>.
- Huerta-Cepas, J., Szklarczyk, D., Heller, D., Hernández-Plaza, A., Forslund, S.K., Cook, H., Mende, D.R., Letunic, I., Rattei, T., Jensen, L.J., von Mering, C., Bork, P., 2019. eggNOG 5.0: a hierarchical, functionally and phylogenetically annotated orthology resource based on 5090 organisms and 2502 viruses. *Nucleic Acids Res.* 47 (D1), D309–D314. <https://doi.org/10.1093/nar/gky1085>.
- Jones, P., Binns, D., Chang, H.Y., Fraser, M., Li, W., Mcanulla, C., McWilliam, H., Maslen, J., Mitchell, A., Nuka, G., Pesseat, S., Quinn, A.F., Sangrador-Vegas, A., Scheremetjev, M., Yong, S.Y., Lopez, R., Hunter, S., 2014. InterProScan 5: genome-scale protein function classification. *Bioinformatics* 30 (9), 1236–1240. <https://doi.org/10.1093/bioinformatics/btu031>.
- Kalvari, I., Nawrocki, E.P., Argasinska, J., Quinones-Olvera, N., Finn, R.D., Bateman, A., Petrov, A.I., 2018. Non-coding RNA analysis using the Rfam database. *Curr. Protoc. Bioinformatics* 62 (1), e51. <https://doi.org/10.1002/cpbi.51>.
- Kanehisa, M., Furumichi, M., Tanabe, M., Sato, Y., Morishima, K., 2017. KEGG: new perspectives on genomes, pathways, diseases and drugs. *Nucleic Acids Res.* 45 (D1), D353–D361. <https://doi.org/10.1093/nar/gkw1092>.
- Katoh, K., Standley, D.M., 2013. MAFFT multiple sequence alignment software version 7: improvements in performance and usability. *Mol. Biol. Evol.* 30 (4), 772–780. <https://doi.org/10.1093/molbev/mst010>.
- Kenny, N.J., McCarthy, S.A., Dudchenko, O., James, K., Betteridge, E., Corton, C., Dolan, J., Mead, D., Oliver, K., Omer, A.D., Pelan, S., Ryan, Y., Sims, Y., Skelton, J., Smith, M., Torrance, J., Weisz, D., Wipat, A., Aiden, E.L., Howe, K., Williams, S.T., 2020. The gene-rich genome of the scallop *Pecten maximus*. *GigaScience* 9 (5). <https://doi.org/10.1093/gigascience/giaa037>.
- Kim, D., Langmead, B., Salzberg, S.L., 2015. HISAT: a fast spliced aligner with low memory requirements. *Nat. Methods* 12 (4), 357–360. <https://doi.org/10.1038/nmeth.3317>.
- Kovaka, S., Zimin, A.V., Pertea, G.M., Razaghi, R., Salzberg, S.L., Pertea, M., 2019. Transcriptome assembly from long-read RNA-seq alignments with StringTie2. *Genome Biol.* 20 (1) <https://doi.org/10.1186/s13059-019-1910-1>.
- Kumar, S., Stecher, G., Suleski, M., Hedges, S.B., 2017. TimeTree: a resource for timelines, timetrees, and divergence times. *Mol. Biol. Evol.* 34 (7), 1812–1819. <https://doi.org/10.1093/molbev/msx116>.
- Li, H., Durbin, R., 2011. Inference of human population history from individual whole-genome sequences. *Nature* 475 (7357), 493–496. <https://doi.org/10.1038/nature10231>.
- Li, H., 2021. New strategies to improve minimap2 alignment accuracy. *Bioinformatics* 37 (23), 4572–4574. <https://doi.org/10.1093/bioinformatics/btab705>.
- Li, A., Dai, H., Guo, X., Zhang, Z., Zhang, K., Wang, C., Wang, X., Wang, W., Chen, H., Li, X., Zheng, H., Li, L., Zhang, G., 2021a. Genome of the estuarine oyster provides insights into climate impact and adaptive plasticity. *Commun. Biol.* 4 (1) <https://doi.org/10.1038/s42003-021-02823-6>.
- Li, H., Durbin, R., 2009. Fast and accurate short read alignment with Burrows-Wheeler transform. *Bioinformatics* 25, 1754–1760. <https://doi.org/10.1093/bioinformatics/btp324>.
- Li, H., Handsaker, B., Wysoker, A., Fennell, T., Ruan, J., Homer, N., Marth, G., Abecasis, G., Durbin, R., 2009. The sequence alignment/map format and SAMtools. *Bioinformatics* 25, 2078–2079. <https://doi.org/10.1093/bioinformatics/btp352>.
- Li, C., Kou, Q., Zhang, Z., Hu, L., Huang, W., Cui, Z., Liu, Y., Ma, P., Wang, H., 2021b. Reconstruction of the evolutionary biogeography reveal the origins and diversification of oysters (Bivalvia: Ostreidae). *Mol. Phylogenet. Evol.* 164, 107268 <https://doi.org/10.1016/j.ympev.2021.107268>.
- Li, L., Li, A., Song, K., Meng, J., Guo, X., Li, S., Li, C., De Wit, P., Que, H., Wu, F., Wang, W., Qi, H., Xu, F., Cong, R., Huang, B., Li, Y., Wang, T., Tang, X., Liu, S., Li, B., Shi, R., Liu, Y., Bu, C., Zhang, C., He, W., Zhao, S., Li, H., Zhang, S., Zhang, L., Zhang, G., 2018. Divergence and plasticity shape adaptive potential of the Pacific oyster. *Nat. Ecol. Evol.* 2 (11), 1751–1760. <https://doi.org/10.1038/s41559-018-0668-2>.

- Li, Y., Sun, X., Hu, X., Xun, X., Zhang, J., Guo, X., Jiao, W., Zhang, L., Liu, W., Wang, J., Li, J., Sun, Y., Miao, Y., Zhang, X., Cheng, T., Xu, G., Fu, X., Wang, Y., Yu, X., Huang, X., Lu, W., Lv, J., Mu, C., Wang, D., Li, X., Xia, Y., Li, Y., Yang, Z., Wang, F., Zhang, L., Xing, Q., Dou, H., Ning, X., Dou, J., Li, Y., Kong, D., Liu, Y., Jiang, Z., Li, R., Wang, S., Bao, Z., 2017. Scallop genome reveals molecular adaptations to semi-sessile life and neurotoxins. *Nat. Commun.* 8 (1) <https://doi.org/10.1038/s41467-017-01927-0>.
- Liu, B., Shi, Y., Yuan, J., Hu, X., Zhang, H., Li, N., Fan, W., 2013. Estimation of Genomic Characteristics by Analyzing k-mer Frequency in De Novo Genome Projects. *arXiv.org*. <https://doi.org/10.48550/arXiv.1308.2012> arXiv: 1308.2012.
- Ludt, W.B., Rocha, L.A., 2015. Shifting seas: the impacts of Pleistocene sea-level fluctuations on the evolution of tropical marine taxa. *J. Biogeogr.* 42 (1), 25–38. <https://doi.org/10.1111/jbi.12416>.
- Manni, M., Berkeley, M.R., Seppy, M., Zdobnov, E.M., 2021. BUSCO: assessing genomic data quality and beyond. *Curr. Protoc. 1* (12) <https://doi.org/10.1002/cpz1.323>.
- Marçais, G., Kingsford, C., 2011. A fast, lock-free approach for efficient parallel counting of occurrences of k-mers. *Bioinformatics* 27 (6), 764–770. <https://doi.org/10.1093/bioinformatics/btr011>.
- Mardones-Toledo, D.A., Montory, J.A., Joyce, A., Thompson, R.J., Diederich, C.M., Pechenik, J.A., Mardones, M.L., Chaparro, O.R., 2015. Brooding in the Chilean oyster *Ostrea chilensis*: Unexpected complexity in the movements of brooded offspring within the mantle cavity. *PLoS One* 10 (4), e122859. <https://doi.org/10.1371/journal.pone.0122859>.
- McCartney, M.A., Auch, B., Kono, T., Mallez, S., Zhang, Y., Obille, A., Becker, A., Abrahante, J.E., Garbe, J., Badalamenti, J.P., Herman, A., Mangelson, H., Liachko, I., Sullivan, S., Sone, E.D., Koren, S., Silverstein, K.A.T., Beckman, K.B., Gohl, D.M., 2022. The genome of the zebra mussel, *Dreissena polymorpha*: a resource for comparative genomics, invasion genetics, and biocontrol. *G3 (Bethesda, Md.)* 12 (2). <https://doi.org/10.1093/g3journal/jkab423>.
- McDowell, I.C., Nikapitiya, C., Aguiar, D., Lane, C.E., Istrail, S., Gomez-Chiarri, M., 2014. Transcriptome of American oysters, *Crassostrea virginica*, in response to bacterial challenge: insights into potential mechanisms of disease resistance. *PLoS One* 9 (8), e105097. <https://doi.org/10.1371/journal.pone.0105097>.
- Mendes, F.K., Vanderpool, D., Fulton, B., Hahn, M.W., 2020. CAFE 5 models variation in evolutionary rates among gene families. *Bioinformatics* 36 (22–23), 5516–5518. <https://doi.org/10.1093/bioinformatics/btaa1022>.
- Minh, B.Q., Schmidt, H.A., Chernomor, O., Schrempf, D., Woodhams, M.D., von Haeseler, A., Lanfear, R., 2020. IQ-TREE 2: new models and efficient methods for phylogenetic inference in the genomic era. *Mol. Biol. Evol.* 37 (5), 1530–1534. <https://doi.org/10.1093/molbev/msaa015>.
- Mistry, J., Chuguransky, S., Williams, L., Qureshi, M., Salazar, G.A., Sonnhammer, E.L.L., Tosatto, S.C.E., Paladini, L., Raj, S., Richardson, L.J., Finn, R.D., Bateman, A., 2021. Pfam: the protein families database in 2021. *Nucleic Acids Res.* 49 (D1), D412–D419. <https://doi.org/10.1093/nar/gkaa913>.
- Morga, B., Renault, T., Faury, N., Chollet, B., Arzul, I., 2011. Cellular and molecular responses of haemocytes from *Ostrea edulis* during in vitro infection by the parasite *Bonamia ostreae*. *Int. J. Parasitol.* 41 (7), 755–764. <https://doi.org/10.1016/j.ijpara.2011.01.013>.
- Nawrocki, E.P., Eddy, S.R., 2013. Infernal 1.1: 100-fold faster RNA homology searches. *Bioinformatics* 29 (22), 2933–2935. <https://doi.org/10.1093/bioinformatics/btt509>.
- Pardo, B.G., Álvarez-Dios, J.A., Cao, A., Ramilo, A., Gómez-Tato, A., Planas, J.V., Villalba, A., Martínez, P., 2016. Construction of an *Ostrea edulis* database from genomic and expressed sequence tags (ESTs) obtained from *Bonamia ostreae* infected haemocytes: development of an immune-enriched oligo-microarray. *Fish Shellfish Immunol.* 59, 331–344. <https://doi.org/10.1016/j.fsi.2016.10.047>.
- Peñalzo, C., Gutierrez, A.P., Eöry, L., Wang, S., Guo, X., Archibald, A.L., Bean, T.P., Houston, R.D., 2021. A chromosome-level genome assembly for the Pacific oyster *Crassostrea gigas*. *GigaScience* 10 (3). <https://doi.org/10.1093/gigascience/giab020>.
- Perrigault, M., Tanguy, A., Allam, B., 2009. Identification and expression of differentially expressed genes in the hard clam, *Mercenaria mercenaria*, in response to quahog parasite unknown (QPX). *BMC Genomics* 10, 377. <https://doi.org/10.1186/1471-2164-10-377>.
- Powell, D., Subramanian, S., Suwansa-Ard, S., Zhao, M., O'Connor, W., Raftos, D., Elizur, A., 2018. The genome of the oyster *Saccostrea* offers insight into the environmental resilience of bivalves. *DNA Res.* 25 (6), 655–665. <https://doi.org/10.1093/dnares/dsy032>.
- Price, M.N., Dehal, P.S., Arkin, A.P., Lab, Lawrence Berkeley National, Lbnl, B.C.U.S., Poon, A.F.Y., 2010. FastTree 2—approximately maximum-likelihood trees for large alignments. *PLoS One* 5 (3), e9490. <https://doi.org/10.1371/journal.pone.0009490>.
- Qi, H., Li, L., Zhang, G., 2021. Construction of a chromosome-level genome and variation map for the Pacific oyster *Crassostrea gigas*. *Mol. Ecol. Resour.* <https://doi.org/10.1111/1755-0998.13368>.
- Rao, S.S., Huntley, M.H., Durand, N.C., Stamenova, E.K., Bochkov, I.D., Robinson, J.T., Sanborn, A.L., Machol, I., Omer, A.D., Lander, E.S., Aiden, E.L., 2014. A 3D map of the human genome at kilobase resolution reveals principles of chromatin looping. *Cell* 159 (7), 1665. <https://doi.org/10.1016/j.cell.2014.11.021>.
- Renault, T., Faury, N., Barbosa-Solomieu, V., Moreau, K., 2011. Suppression subtractive hybridisation (SSH) and real time PCR reveal differential gene expression in the Pacific cupped oyster, *Crassostrea gigas*, challenged with *Ostreid herpesvirus 1*. *Dev. Comp. Immunol.* 35 (7), 725–735. <https://doi.org/10.1016/j.dci.2011.02.004>.
- Rodríguez-Juiz, A.M., Torrado, M., Méndez, J., 1996. Genome-size variation in bivalve molluscs determined by flow cytometry. *Mar. Biol.* 126 (3), 489–497. <https://doi.org/10.1007/BF00354631>.
- Rogers, R.L., Grizzard, S.L., Titus McQuillan, J.E., Bockrath, K., Patel, S., Wares, J.P., Garner, J.T., Moore, C.C., 2021. Gene family amplification facilitates adaptation in freshwater unionid bivalve *Megalania nervosa*. *Mol. Ecol.* 30 (5), 1155–1173. <https://doi.org/10.1111/mec.15786>.
- Ronza, P., Cao, A., Robledo, D., Gómez-Tato, A., Álvarez-Dios, J.A., Hasanuzzaman, A.F.M., Quiroga, M.I., Villalba, A., Pardo, B.G., Martínez, P., 2018. Long-term affected flat oyster (*Ostrea edulis*) haemocytes show differential gene expression profiles from naive oysters in response to *Bonamia ostreae*. *Genomics* 110 (6), 390–398. <https://doi.org/10.1016/j.ygeno.2018.04.002>.
- Sigwart, J.D., Lindberg, D.R., Chen, C., Sun, J., 2021. Molluscan phylogenomics requires strategically selected genomes. *Philos. Trans. R. Soc. B* 376 (1825), 20200161. <https://doi.org/10.1098/rstb.2020.0161>.
- Simakov, O., Marletaz, F., Cho, S., Edsinger-Gonzales, E., Havlak, P., Hellsten, U., Kuo, D., Larsson, T., Lv, J., Arendt, D., Savage, R., Osoegawa, K., de Jong, P., Grimwood, J., Chapman, J.A., Shapiro, H., Aerts, A., Olliar, R.P., Terry, A.Y., Boore, J.L., Grigoriev, I.V., Lindberg, D.R., Seaver, E.C., Weisblat, D.A., Putnam, N.H., Rokhsar, D.S., 2013. Insights into bilaterian evolution from three spiralian genomes. *Nature* 493 (7433), 526–531. <https://doi.org/10.1038/nature11696>.
- Slotkin, R.K., Martienssen, R., 2007. Transposable elements and the epigenetic regulation of the genome. *Nat. Rev. Genet.* 8 (4), 272–285. <https://doi.org/10.1038/nrg2072>.
- Stanke, M., Diekhans, M., Baertsch, R., Haussler, D., 2008. Using native and syntentically mapped cDNA alignments to improve de novo gene finding. *Bioinformatics* 24 (5), 637–644. <https://doi.org/10.1093/bioinformatics/btn013>.
- Sun, J., Mu, H., Ip, J.C.H., Li, R., Xu, T., Accorsi, A., Sánchez Alvarado, A., Ross, E., Lan, Y., Sun, Y., Castro-Vazquez, A., Vega, I.A., Heras, H., Ituarte, S., Van Bocxlaer, B., Hayes, K.A., Cowie, R.H., Zhao, Z., Zhang, Y., Qian, P., Qiu, J., 2019. Signatures of Divergence, Invasiveness, and Terrestrialization Revealed by Four Apple Snail Genomes. *Mol. Biol. Evol.* 36 (7), 1507–1520. <https://doi.org/10.1093/molbev/msz084>.
- Sun, J., Li, R., Chen, C., Sigwart, J.D., Kocot, K.M., 2021. Benchmarking Oxford Nanopore read assemblers for high-quality molluscan genomes. *Philos. Trans. R. Soc. B*. <https://doi.org/10.6084/m9.figshare>.
- Tanguy, A., Guo, X., Ford, S.E., 2004. Discovery of genes expressed in response to *Perkinsus marinus* challenge in Eastern (*Crassostrea virginica*) and Pacific (*C. gigas*) oysters. *Gene* 338 (1), 121–131. <https://doi.org/10.1016/j.gene.2004.05.019>.
- Tarailo-Graovac, M., Chen, N., 2009. Using RepeatMasker to identify repetitive elements in genomic sequences. *Curr. Protoc. Bioinformatics* 25 (1), 4.10.11–4.10.14. <https://doi.org/10.1002/0471250953.bi0410s25>.
- Thiriou-Quévieux, C., Insua, A., 1992. Nuclear organizer region variation in the chromosomes of three oyster species. *J. Exp. Mar. Biol. Ecol.* 157 (1), 33–40. [https://doi.org/10.1016/0022-0981\(92\)90072-1](https://doi.org/10.1016/0022-0981(92)90072-1).
- Tsang, L.M., Wu, T.H., Shih, H., Williams, G.A., Chu, K.H., Chan, B.K.K., 2012. Genetic and morphological differentiation of the Indo-West Pacific intertidal barnacle *Chthamalus malayensis*. *Integr. Comp. Biol.* 52 (3), 388–409. <https://doi.org/10.1093/icb/ics044>.
- Varney, R.M., Speiser, D.I., McDougall, C., Degnan, B.M., Kocot, K.M., 2021. The iron-responsive genome of the chiton *Acanthopleura granulata*. *Genome Biol. Evol.* 13 (1) <https://doi.org/10.1093/gbe/evaa263>.
- Vera, M., Pardo, B.G., Cao, A., Vilas, R., Fernández, C., Blanco, A., Gutierrez, A.P., Bean, T.P., Houston, R.D., Villalba, A., Martínez, P., 2019. Signatures of selection for bonamiosis resistance in European flat oyster (*Ostrea edulis*): New genomic tools for breeding programs and management of natural resources. *Evol. Appl.* 12 (9), 1781–1796. <https://doi.org/10.1111/eva.12832>.
- Wang, K., Wang, J., Zhu, C., Yang, L., Ren, Y., Ruan, J., Fan, G., Hu, J., Xu, W., Bi, X., Zhu, Y., Song, Y., Chen, H., Ma, T., Zhao, R., Jiang, H., Zhang, B., Feng, C., Yuan, Y., Gan, X., Li, Y., Zeng, H., Liu, Q., Zhang, Y., Shao, F., Hao, S., Zhang, H., Xu, X., Liu, X., Wang, D., Zhu, M., Zhang, G., Zhao, W., Qiu, Q., He, S., Wang, W., 2021. African lungfish genome sheds light on the vertebrate water-to-land transition. *Cell*. <https://doi.org/10.1016/j.cell.2021.01.047>.
- Wang, S., Zhang, J., Jiao, W., Li, J., Xun, X., Sun, Y., Guo, X., Huan, P., Dong, B., Zhang, L., Hu, X., Sun, X., Wang, J., Zhao, C., Wang, Y., Wang, D., Huang, X., Wang, R., Lv, J., Li, Y., Zhang, Z., Liu, B., Lu, W., Hui, Y., Liang, J., Zhou, Z., Hou, R., Li, X., Liu, Y., Li, H., Ning, X., Lin, Y., Zhao, L., Xing, Q., Dou, J., Li, Y., Mao, J., Guo, H., Dou, H., Li, T., Mu, C., Jiang, W., Fu, Q., Fu, X., Miao, Y., Liu, J., Yu, Q., Li, R., Liao, H., Li, X., Kong, Y., Jiang, Z., Chourrout, D., Li, R., Bao, Z., 2017. Scallop genome provides insights into evolution of bilaterian karyotype and development. *Nat. Ecol. Evol.* 1 (5), 120. <https://doi.org/10.1038/s41559-017-0120>.
- Wang, L., Song, X., Song, L., 2018b. The oyster immunity. *Dev. Comp. Immunol.* 80, 99–118. <https://doi.org/10.1016/j.dci.2017.05.025>.
- Wang, W., Song, X., Wang, L., Song, L., 2018a. Pathogen-derived carbohydrate recognition in molluscs immune defense. *Int. J. Mol. Sci.* 19 (3), 721. <https://doi.org/10.3390/ijms19030721>.
- Wang, Y., Tang, H., Debarry, J.D., Tan, X., Li, J., Wang, X., Lee, T., Jin, H., Marler, B., Guo, H., Kissinging, J.C., Paterson, A.H., 2012. MCScanX: a toolkit for detection and evolutionary analysis of gene synteny and collinearity. *Nucleic Acids Res.* 40 (7), e49. <https://doi.org/10.1093/nar/gkr1293>.
- Wanninger, A., Wollesen, T., 2019. The evolution of molluscs. *Biol. Rev.* 94 (1), 102–115. <https://doi.org/10.1111/brv.12439>.
- Wheeler, T.J., Clements, J., Eddy, S.R., Hubley, R., Jones, T.A., Jurka, J., Smit, A.F., Finn, R.D., 2012. Dfam: a database of repetitive DNA based on profile hidden Markov models. *Nucleic Acids Res.* 41 (D1), D70–D82. <https://doi.org/10.1093/nar/gks1265>.
- Witkop, E.M., Proestou, D.A., Gomez-Chiarri, M., 2022. The expanded inhibitor of apoptosis gene family in oysters possesses novel domain architectures and may play diverse roles in apoptosis following immune challenge. *BMC Genomics* 23 (1) <https://doi.org/10.1186/s12864-021-08233-6>.

- Yan, X., Nie, H., Huo, Z., Ding, J., Li, Z., Yan, L., Jiang, L., Mu, Z., Wang, H., Meng, X., Chen, P., Zhou, M., Rbbani, M.G., Liu, G., Li, D., 2019. Clam genome sequence clarifies the molecular basis of its benthic adaptation and extraordinary shell color diversity. *iScience* 19, 1225–1237. <https://doi.org/10.1016/j.isci.2019.08.049>.
- Yang, J.L., Feng, D.D., Liu, J., Xu, J.K., Chen, K., Li, Y.F., Liang, X., Lu, Y., 2021. Chromosome-level genome assembly of the hard-shelled mussel *Mytilus coruscus*, a widely distributed species from the temperate areas of East Asia. *GigaScience* 10 (4), giab024. <https://doi.org/10.1093/gigascience/giab024>.
- Yang, Z., 2007. PAML 4: phylogenetic analysis by maximum likelihood. *Mol. Biol. Evol.* 24 (8), 1586–1591. <https://doi.org/10.1093/molbev/msm088>.
- Yang, Z., Zhang, L., Hu, J., Wang, J., Bao, Z., Wang, S., 2020. The evo-devo of molluscs: Insights from a genomic perspective. *Evol. Dev.* 22 (6), 409–424. <https://doi.org/10.1111/ede.12336>.
- Yu, G., Wang, L.G., Han, Y., He, Q.Y., 2012. CLUSTERPROFILER: an R package for comparing biological themes among gene clusters. *OMICS* 16 (5), 284–287. <https://doi.org/10.1089/omi.2011.0118>.
- Zhang, Y., Mao, F., Mu, H., Huang, M., Bao, Y., Wang, L., Wong, N., Xiao, S., Dai, H., Xiang, Z., Ma, M., Xiong, Y., Zhang, Z., Zhang, L., Song, X., Wang, F., Mu, X., Li, J., Ma, H., Zhang, Y., Zheng, H., Simakov, O., Yu, Z., 2021. The genome of *Nautilus pompilius* illuminates eye evolution and biomineralization. *Nat. Ecol. Evol.* 5 (7), 927–938. <https://doi.org/10.1038/s41559-021-01448-6>.
- Zhang, Y., Mao, F., Xiao, S., Yu, H., Xiang, Z., Xu, F., Li, J., Wang, L., Xiong, Y., Chen, M., Bao, Y., Deng, Y., Huo, Q., Zhang, L., Liu, W., Li, X., Ma, H., Zhang, Y., Mu, X., Liu, M., Zheng, H.K., Wong, N.K., Yu, Z., 2022. Comparative genomics reveals evolutionary drivers of sessile life and left-right shell asymmetry in bivalves. *Genom. Proteom. Bioinf.* <https://doi.org/10.1016/j.gpb.2021.10.005>.